Adaption and recovery of Nitrosomonas europaea to chronic TiO_2 nanoparticle exposure

Wu, Junkang; Zhan, Manjun; Chang, Yan; Su, Qingxian; Yu, Ran

Published in:
Water Research

Link to article, DOI:
10.1016/j.watres.2018.09.043

Publication date:
2018

Document Version
Peer reviewed version

Accepted Manuscript

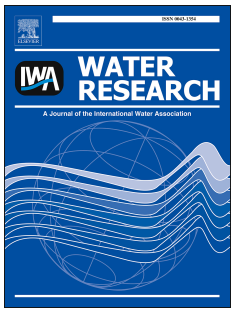

Adaption and recovery of *Nitrosomonas europaea* to chronic TiO_2 nanoparticle exposure

Junkang Wu, Manjun Zhan, Yan Chang, Qingxian Su, Ran Yu

PII: S0043-1354(18)30758-9

DOI: 10.1016/j.watres.2018.09.043

Reference: WR 14093

To appear in: *Water Research*

Received Date: 18 May 2018

Revised Date: 24 September 2018

Accepted Date: 25 September 2018

Please cite this article as: Wu, J., Zhan, M., Chang, Y., Su, Q., Yu, R., Adaption and recovery of *Nitrosomonas europaea* to chronic TiO_2 nanoparticle exposure, *Water Research* (2018), doi: https://doi.org/10.1016/j.watres.2018.09.043.

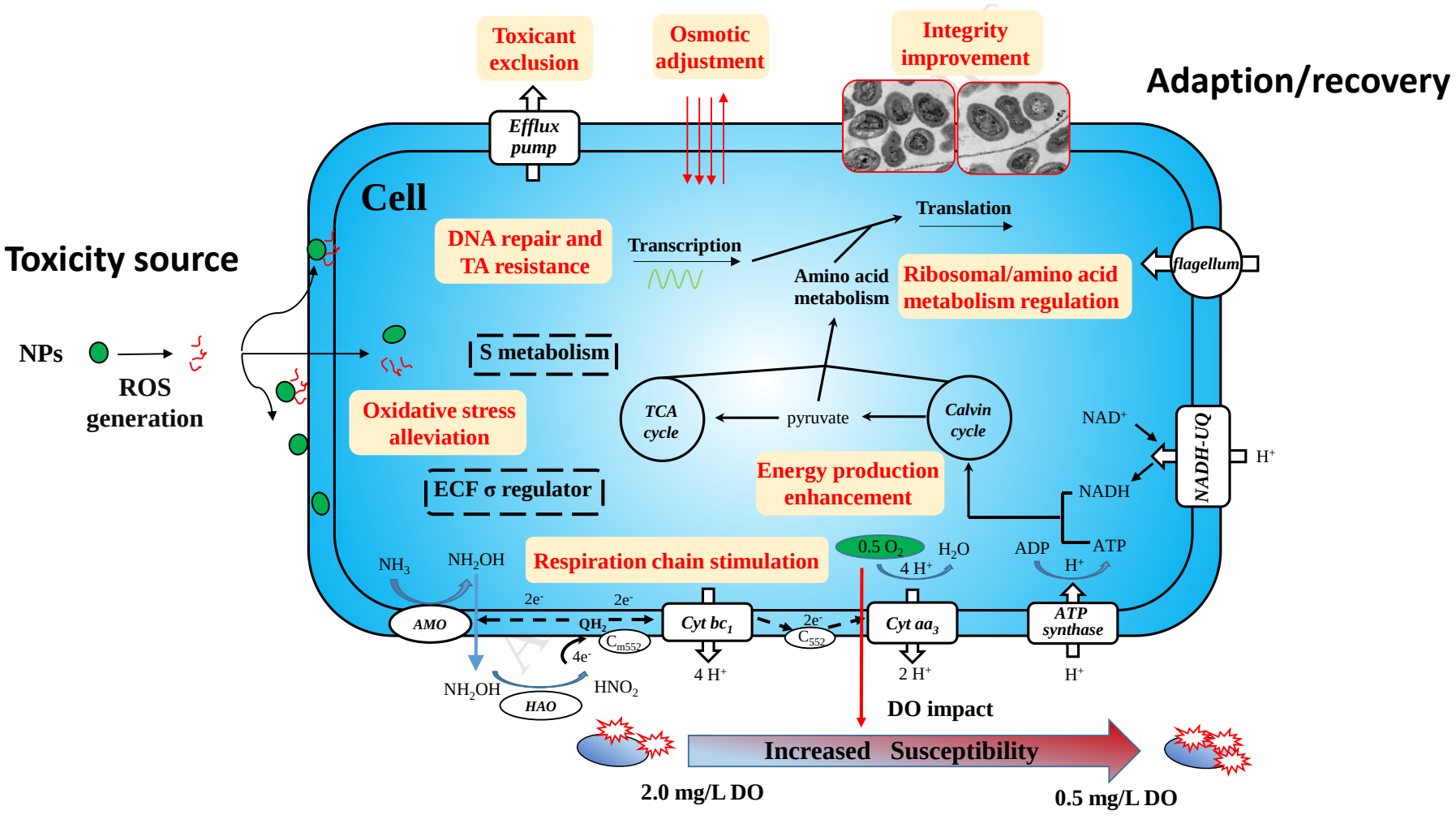
Toxicant exclusion
Osmotic adjustment
Integrity improvement
Adaption/recovery
Efflux pump
Cell
Toxicity source
NPs
ROS generation
DNA repair and TA resistance
Transcription
Translation
Amino acid metabolism
Ribosomal/amino acid metabolism regulation
flagellum
S metabolism
Oxidative stress alleviation
TCA cycle
pyruvate
Calvin cycle
NAD+
NADH-UQ
H+
NADH
ECF σ regulator
Energy production enhancement
Respiration chain stimulation
0.5 O2
H2O
4 H+
ADP
ATP
H+
NH3
NH2OH
2e-
2e-
AMO
QH2
Cm552
Cyt bc1
2e-
C552
Cyt aa3
ATP synthase
4e-
4 H+
2 H+
H+
NH2OH
HAO
HNO2
DO impact
Increased Susceptibility
2.0 mg/L DO
0.5 mg/L DO

TITLE PAGE

Adaption and recovery of *Nitrosomonas europaea* to chronic TiO_2 nanoparticle exposure

Junkang Wu[1,2,3], Manjun Zhan[4], Yan Chang[1,2], Qingxian Su[3], Ran Yu*[1,2]

1. Department of Environmental Science and Engineering, School of Energy and Environment, Wuxi Engineering Research Center of Taihu Lake Water Environment, Southeast University, Nanjing, Jiangsu, China 210096

2. Key Laboratory of Environmental Medicine Engineering, Ministry of Education, Southeast University, Nanjing, Jiangsu, China 210009

3. Department of Environmental Engineering, Technical University of Denmark, Lyngby, Denmark 2800

4. Nanjing Research Institute of Environmental Protection, Nanjing Environmental Protection Bureau, Nanjing, Jiangsu, China 210013

* Corresponding author:

Ran Yu, Department of Environmental Science and Engineering, School of Energy and Environment, Southeast University, No.2 Sipailou Street, Nanjing, 210096, China; Phone: (+86) 15312083786; Fax: (+86) 25 83792614; email: yuran@seu.edu.cn

Abstract: Although the adverse impacts of emerging nanoparticles (NPs) on the biological nitrogen removal (BNR) process have been broadly reported, the adaptive responses of NP-impaired nitrifiers and the related mechanisms have seldom been addressed to date. Here, we systematically explored the adaption and recovery capacities of the ammonia oxidizer *Nitrosomonas europae*a under chronic TiO_2 NP exposure and different dissolved oxygen (DO) conditions at the physiological and transcriptional levels in a chemostat reactor. *N. europae*a cells adapted to 50 mg/L TiO_2 NP exposure after 40-d incubation and the inhibited cell growth, membrane integrity, nitritation rate, and ammonia monooxygenase activity all recovered regardless of the DO concentrations. Transmission electron microscope imaging indicated the remission of the membrane distortion after the cells' 40-d adaption to the NP exposure. The microarray results further suggested that the metabolic processes associated with the membrane repair were pivotal for cellular adaption/recovery, such as the membrane efflux for toxicant exclusion, the structural preservation or stabilization, and the osmotic equilibrium adjustment. In addition, diverse metabolic and stress-defense pathways, including aminoacyl-tRNA biosynthesis, respiratory chain, ATP production, toxin-antitoxin 'stress-fighting', and DNA repair were activated for the cellular adaption coupled with the metabolic activity recovery, probably via recovering the energy production/conversion efficiency and mediating the non-photooxidative stress. Finally, low DO (0.5 mg/L) incubated cells were more susceptible to TiO_2 NP exposure and required more time to adapt to and recover from the stress, which was probably due to the stimulation limitation of the oxygen-dependent energy metabolism with a lower oxygen supply. The findings of this study provide new insights into NP contamination control and management adjustments during the BNR process.

Keywords: TiO_2 nanoparticle; *Nitrosomonas europae*a; dissolved oxygen; adaption;

26 microarray

1 Introduction

Metal oxide nanomaterials characterized by sizes smaller than 100 nm in at least one dimension are extensively used in many commercial and industrial fields owing to their unique physico-chemical properties (Vance et al. 2015). Titanium oxide nanoparticles (TiO_2 NPs) with high photocatalytic, ultraviolet shielding, and antibacterial activities are widely found in cosmetics, textiles, sunscreens, photo-catalysts, and lithium batteries (Minetto et al. 2014). TiO_2 NPs are the most widely used nanomaterials worldwide and their production has rapidly increased to 10,000 tons per year during 2011–2014 (Piccinno et al. 2012) and is expected to reach 2.5 million tons per year by 2025 (Robichaud et al. 2009). Due to their extensive application, TiO_2 NPs are inevitably released into the environment and are recognized as an emerging environmental stressor (Gondikas et al. 2014). As a result, the negative impacts of TiO_2 NPs on animal cells (Yu et al. 2017), aquatic organisms (Hu et al. 2017), bacterial cells (Liu et al. 2016), plants (Zahra et al. 2017) , and biofilm communities (Binh et al. 2016) have been widely recognized and have raised increasing concerns regarding their biosafety and biosecurity in ecosystems.

Recently, the release of engineered TiO_2 NPs into biological wastewater treatment plants (WWTPs) has drawn significant attention (Polesel et al. 2018; Zhou et al. 2015). TiO_2 NP associated Ti concentrations of 181 - 1233 µg/L were detected in the raw sewage of 10 representative WWTPs in the US (Westerhoff et al. 2011). The TiO_2 NP concentrations in the effluents of European WWTP were estimated to have increased from 2.5–10.8 µg/L in 2009 to 13–110 µg/L in 2013 (Sun et al. 2014; Gottschalk et al. 2009). The increased production and usage of TiO_2 NPs will inevitably cause the occurrence of higher NP concentrations in WWTPs in the near future. As a result, the diverse microorganisms used for pollutant removal in WWTPs are potentially threatened by the TiO_2 NPs due to their bio-toxicities. TiO_2 NPs have been reported to reduce the bacterial abundances or microbial community diversities, depress the activities of ammonia monooxygenase (AMO), nitrite oxidoreductase, exopolyphosphatase, and polyphosphate kinase, and thus inhibit organic matter degradation processes and decrease the nitrogen and

phosphorus removal efficiencies in WWTPs (Li et al. 2017; Li et al. 2016; Zhang et al. 2018). The nitrogen removal process is generally more susceptible to NP-caused stress than the phosphorus removal process. During a 70-d operation of a sequencing batch reactor (SBR) with a concentration of 50 mg/L TiO_2 NPs in the influent, the nitrogen removal rate was significantly retarded by 69.6 % whereas the phosphorus removal efficiencies remained constant (Zheng et al. 2011a). As the rate-limiting and first nitrification step in a biological nitrogen removal (BNR) system, the ammonia oxidation process (nitritation) performed by ammonia-oxidizing bacteria (AOB) is vulnerable to NP stress. Zheng et al. (2011a) and Yang et al. (2013) have discovered the high sensitivity of the ammonia oxidation process to TiO_2 or Ag NP-caused stress in the BNR systems.

Currently, the TiO_2 NP toxicity has been acknowledged to be caused by oxidative stress due to the reactive oxygen species (ROS) generation and physical interruption when NPs are adsorbed onto the cell membrane or internalized into the cells (Huang et al. 2017; Li et al. 2012; Liu et al. 2009). Nevertheless, most research studies have mainly focused on the acute or batch exposure effects to cell respiration, microbial diversity, or wastewater treatment performances (Li et al. 2017; Zheng et al. 2011a; Li et al. 2015). Few studies have investigated the mechanisms of the metabolic and transcriptional regulations of nitrifiers in response to chronic TiO_2 NP exposure in a continuous flow bioreactor. In addition, self-adaptive regulations or the self-recovery potential of NP-impaired nitrifiers and the associated mechanisms have been seldom addressed to date, which are crucial for developing emergency adjustment strategies in response to NP-impacted wastewater treatment biosystems. Only our previous study addressed these issues and we discovered the recovery potentials of ZnO NP-impaired AOB and the associated regulation pathways including membrane fixation, heavy metal resistance, toxin-antitoxin defense, and oxidative phosphorylation after 6-h recovery during batch incubation (Wu et al. 2017).

It is noteworthy that AOB are highly sensitive to many environmental factors including dissolved oxygen (DO) levels (Prosser 1990). In addition, we have found that oxygen oxidation-dependent electron transfer pathways were actively involved in the stress response of *N.*

europaea cells to ZnO NP exposure (Wu et al. 2017). Therefore, the DO level could potentially affect the NP toxicity effects to *N. europaea*, which is a typical chemolithotrophic AOB and widely exists in BNR processes (Kowalchuk and Stephen 2001). In this study, we hypothesized that *N. europaea* cells have adaption and recovery capacities in response to chronic TiO_2 NP stress and that the DO level is a key factor affecting their adaption capacities. To test these hypotheses, the physiological and metabolic responses of the continuously cultivated *N. europaea* to chronic TiO_2 NP stress under both aerobic and microaerobic conditions were compared and the recovery capacities of the NP-impaired cells were further assessed. Genome-wide microarray and quantitative reverse-transcriptase polymerase chain reaction (qRT-PCR) techniques were used for the exploration of the transcriptional regulations of the NP-impaired *N. europaea* cells, as well as the associated adaptive regulation and recovery mechanisms.

2 Materials and Methods

2.1 Chemostat bioreactor operation

N. europaea (ATCC 19718) was continuously cultivated in a stirred chemostat bioreactor with a 3 L working volume (hydraulic retention time: 2.2 d) at 25 °C in the dark. The DO concentration was maintained at 2.0 ± 0.2 or 0.5 ± 0.2 mg/L by filter-sterilized air aeration. The pH in the reactor was maintained at 7.50 ± 0.10 by the automatic introduction of a saturated sterilized $NaHCO_3$ buffer with a Meller pH controller (Taiwan, China). The cultivation medium was similar to that used in a previous study (Yu et al. 2015) and contained 10 mM $(NH_4)_2SO_4$, 10 mM 3-[4-(2-Hydroxyethyl)-1-piperazine] propanesulfonic acid, 0.8 mM $MgSO_4 \cdot 7H_2O$, 0.5 mM of K_2HPO_4, 0.1 mM of $CaCl_2 \cdot 2H_2O$, 2.4 μM EDTA-Fe^{3+}, 1 μM $CuSO_4 \cdot 5H_2O$, 0.9 μM of $MnCl_2 \cdot 4H_2O$, 0.4 μM $Na_2MoO_4 \cdot 2H_2O$, 0.3 μM $ZnSO_4 \cdot 7H_2O$, and 0.02 μM $CoCl_2 \cdot 6H_2O$.

2.2 Nanoparticle characterization

The anatase TiO_2 NPs were bought from Sigma Company (St. Louis, MO, USA). A JSM-6390A scanning electron microscope (SEM) (Japan Electronics Co., Ltd, Japan) was used to

characterize the primary size of the NPs. The average hydrodynamic diameter with a refractive index of 1.43 and the ζ potential of the TiO_2 NP suspension in Mill-Q water was determined by dynamic light scattering (DLS) using a Malvern Nano ZS90 analyzer (Malvern, United Kingdom). Prior to the measurements, the TiO_2 NP suspension was subject to ultrasonic dispersion for 15 min (50 kHz, 16 W).

2.3 Exposure experiment setup

The TiO_2 NPs with a concentration of 1 or 50 mg NPs/L were added to the reactor to investigate their chronic impacts on *N. europaea* cultivated either at 0.5 or 2.0 mg DO/L. The 1 mg/L TiO_2 NP concentration was chosen to mimic the environmental-relevant value before entering the WWTPs (Westerhoff et al. 2011). The effects of 50 mg/L NPs on the bioreactor performance were also assessed because the TiO_2 NP concentration may potentially increase in the near future due to the increased production and usage (Robichaud et al. 2009) and to ensure the detectability of the toxicity effects. Prior to the NP exposure experiments, each chemostat reactor was operated for at least four weeks to ensure stable performances as the baseline control. The NH_4^+-N, NO_2^--N, cell density, and AMO activities were monitored every day and were generally around 3 mg/L, 267 mg/L, $3.0*10^8$ cell/mL, and 0.98 μg nitrite/mg protein/min, respectively. At the beginning of the NP exposure experiment, the TiO_2 NPs were introduced to the bioreactor and the influent at the final concentrations of 1 or 50 mg/L respectively. The cultures were sampled at the designated time points (0, 3, 6, 12, and 48 h during the first 2 d, every 2 d during the next 18 d, and every 5 d until the end) throughout the 40-d exposure experiment.

2.4 Analytical procedures

The NH_4^+-N and NO_2^--N concentrations were determined using Standard Methods (SEPAC 2002). The cell concentration was quantified by a direct count with a bacterial counting chamber (Hausser Scientific Partnership, PA, USA) using a Nikon microscope (Nikon, Japan). The cell membrane integrity was examined with a fluorescence test using a LIVE/DEAD® BacLight™ Bacterial Viability Kit (Life Technologies, MA, USA) and following the manufacturer's instructions.

The specific AMO enzyme activity for the ammonia oxidation was determined in terms of nitrite production rate per unit of protein using an optimized reporting method as described previously (Zheng et al. 2011b; Yu et al. 2016).

The cell morphological changes under chronic TiO_2 NP stress (12-d and 40-d exposure) were assessed using a JEM-2100 transmission electron microscope (TEM) (Japan Electronics Co., Ltd, Japan) as described elsewhere (Yu et al. 2016). Briefly, the harvested cell pellets were fixed with 3–5 % glutaraldehyde, dehydrated in 50, 70, 80, and 90 % ethanol (4 °C) and acetone (25 °C) for 20 min in sequence, and finally embedded in resin before sectioning for the TEM observation.

2.5 RNA extraction and microarray-chip analysis

The total RNA was extracted and purified using the RNeasy Mini Kit (Qiagen, Hilden, Germany) and following the manufacturer's instructions. The RNA concentration was quantified with a Nanodrop ND-1000 spectrophotometer (Nanodrop Technologies, Wilmington, DE, USA) and the RNA integrity was assessed using standard denaturing agarose gel electrophoresis. Based on the physiological responses of the *N. europaea* cells after 40-d exposure to the TiO_2 NPs, three triplicate samples, which included the pre-exposure cell sample (Pre.), the 12-d NP-impacted cell sample (Imp.), and the recovered cell sample after 40-d NP exposure (Rec.) were assayed using an oligonucleotide microarray (Agilent Technologies, Palo Alto, CA, USA) with all 2436 annotated transcripts represented in the *N. europaea* ATCC 19718 genome (Chain et al. 2003). The sample labeling and microarray hybridization were conducted following the Agilent One-Color Microarray-Based Gene Expression Analysis protocol (Agilent Technologies, Santa Clara, CA, USA). In brief, the total RNA from each sample was amplified and transcribed into fluorescent cRNA with Cy3-UTP labeled using Agilent's Quick Amp Labeling Kit (version 5.7, Agilent Technologies). The labeled cRNAs were then hybridized onto the *N. europaea* ATCC 19718 Microarray (8x15K, Agilent Technologies) using the Agilent Gene Expression Hybridization Kit. After washing, an Agilent Scanner G2505C (Agilent Technologies) was used to scan the arrays.

The array images were obtained using the Agilent Feature Extraction software (version

11.0.1.1, Agilent Technologies) for the data analysis. The GeneSpring GX v12.0 software (Agilent Technologies) was used for the quantile normalization of the data and subsequent processing. The regulation of the gene expressions was expressed as the fold-change ratio (FC) (log2 transformed) of the normalized signal intensity between the NP-impacted samples and the pre-exposure cells. The identification of the differentially regulated transcripts with a statistical significance level of $|FC| \geq 1.0$, $p \leq 0.05$ was performed using volcano plot filtering (Agilent Technologies). The clusters of the genes' corresponding orthologous groups (COG) and the related pathway analysis were determined using the latest Microbial Genome Annotation and Analysis Platform (https://www.genoscope.cns.fr/agc/microscope/home/index.php) and the Kyoto Encyclopedia of Genes and Genomes database (http://www.genome.jp/kegg/kegg2.html). The microarray data has been submitted to the Gene Expression Omnibus database under accession number GSE111100 (https://www.ncbi.nlm.nih.gov/geo/query/acc.cgi?acc=GSE111100).

2.6 qRT-PCR

Three differentially expressed genes (NE0669, NE0731, and *Rh50*) were screened for the validation of the microarray results using a ViiA 7 Real-time PCR System (Applied Biosystems, USA). The extracted RNA for the microarray hybridization was also used in the qRT-PCR analysis. The specific primers were designed with Primer Premier 5.0 software (Premier Biosoft, Canada) and are listed in Table S1. The analysis procedures were explained in a previous study (Yu et al. 2016). The amplification conditions were: pre-denaturation at 95 °C for 10 min, denaturation at 95 °C for 10 s, and annealing at 60 °C for 60 s (40 cycles). After application, the melting curve was obtained (60–99 °C, ramp rate: 0.05 °C/s) to confirm the non-specific amplicons. Finally, the target gene expressions were normalized to that of the 16S rRNA genes. The 16S rRNA gene expressions were not significantly affected after 12-d ($p = 0.278$) and 40-d ($p = 0.467$) TiO_2 NP exposure using t-test analysis.

2.7 Statistical analysis

Three replicate runs of two chemostats for 1 and 50 mg/L NP exposure were conducted. All the

results are presented as means ± standard deviation (n=3). Independent unpaired two-sample student's t-tests were used to assess significance and the statistical significance level was $p \leq 0.05$.

3 Results

3.1 NP characterization

The average primary particle size of the ellipse-shaped TiO_2 NPs as determined by SEM imaging was 42 ± 11 nm (Fig. S1). The NPs' hydrodynamic size and ζ potential were 187 ± 69 nm and -20.4 ± 2.1 mV, respectively.

3.2 Physiological responses to chronic NP exposure

3.2.1 Changes in cell density, average size, and ζ potential

One mg/L TiO_2 NPs did not induce markedly negative effects on the cells' density (Fig. 1A), size (884 ± 42 nm, Fig. S2A), and ζ potential (-21.3 ± 2.3 mV, Fig. S2B) during the entire 40-d exposure period. When exposed to 50 mg/L TiO_2 NPs, the cell density remained stable for the first 5 d and then significantly decreased ($p = 0.002$) to as low as 48.6 ± 7.8 % of the original value at the end of the 10-d NP exposure (Fig. 1A). However, the cell density gradually approached the original value ($p = 0.140$) after 30-d incubation and finally remained (Fig. 1A). In contrast, the cell size significantly increased and the ζ potential decreased within the first 2 d but both reverted to the original levels although slight fluctuations were observed during the NP exposure period (Fig. S2).

3.2.2 Cell membrane integrity and morphology variations

The cell membrane integrities were first significantly compromised but then recovered from the TiO_2 NP stress at the levels of 1 and 50 mg/L (Fig. 1B). During the 1 mg/L NP exposure period, the cell membrane integrity gradually decreased but finally stabilized at 96.1 %. In contrast, at 50 mg/L NP, the cell membrane integrity progressively recovered from the lowest value of 88.4 ± 0.7 % (~12 d) to around 96 % at the end of the 30-d NP exposure period (Fig. 1B). The cell morphology changes were further examined using TEM imaging. The average lengths of the pre-exposure cells (Fig. 2A), the 12-d NP-impacted cells (Fig. 2B), and the 40-d NP-impacted cells (Fig. 2C) were

0.928 ± 0.153, 0.851 ± 0.131, and 0.859 ± 0.141 µm (n=10) and the widths were 0.630 ± 0.066, 0.581 ± 0.076, and 0.590 ± 0.103 µm (n=10), respectively. There were no significant differences in the lengths and widths between the treatments ($p \leq 0.05$) despite a slight decrease after the NP exposure. The pre-exposure cells without NP impact exhibited a clear and intact membrane structure (Fig. 2A). After 12-d exposure to 50 mg/L TiO_2 NPs, the cell's multilayer membrane structure was strongly distorted and deformed or even became undistinguishable (Fig. 2B). This was consistent with the observed strongly impaired membrane integrity (Fig. 1B). However, after prolonged NP stress (40 d), the membrane integrity improvement of about 60–75% reflected the alleviation of the cell deformation (Fig. 2C), which indicated the cells' potential adaptive adjustment and membrane preservation ability under chronic TiO_2 NPs stress.

3.2.3 NP impacts on the nitritation performances and AMO activity

The ammonium and nitrite concentrations in the bioreactor were not noticeably affected during the long-term exposure to 1 mg/L TiO_2 NPs, whereas 50 mg/L TiO_2 NPs induced a significant decrease in the nitritation rate ($p = 0.013$) and thus the accumulation of ammonium and a reduction in the nitrite concentration in the bioreactor after 6-d of NP stress (Fig. 3A-B). The specific AMO activity exhibited a similar trend under 1 or 50 mg/L TiO_2 NP stress (Fig. 3C) as the ammonium and nitrite concentrations. The maximal reductions in the nitritation rate and AMO activity were 5.6 ± 0.8 % and 30.0 ± 1.7 %, respectively at 50 mg/L NP stress for approximate 12 d (Fig. 3). However, the nitritation performance eventually recovered to the original level and remained stable (Fig. 3A-B). In addition, the cells regained the specific AMO activity close to the original level with no significant differences ($p = 0.094$) (Fig. 3C), which was in agreement with the recovery potential of the cell density (Fig. 1A), the membrane integrity (Fig. 1B), and the nitritation performance (Fig. 3A-B).

3.2.4 Effects of DO on chronic NP toxicities

Unlike the responses to the DO concentration of 2 mg/L, the cell growth, membrane integrity, nitritation performance, and AMO activity were immediately depressed when treated with NPs at a

low DO level of 0.5 mg/L (Fig. 1 & 3) despite the unremarkable changes in cell size and ζ potential (Fig. S2). In addition, the inhibition rates of all the metabolic activities of *N. europaea* were much higher in the low-DO cultured cells than in the cells cultured at 2 mg DO/L after 6-h NP exposure (Fig. 1 & 3). However, the DO level did not affect the recovery potentials of the NP-impaired cells because the cells finally regained their metabolic activities and reached nearly the same levels as the normal cells despite the prolonged adaptation time for the low-DO cultured cells. Therefore, *N. europaea* cells displayed a DO-independent recoverability when long-term exposed to TiO_2 NPs and the high DO condition benefited the cells' resistance to NP stress and shortened the cells' NP toxicity adaptation and recovery time of the metabolic activity.

3.3 Transcriptional profiling

In comparison to the pre-exposure cells, 269 and 193 transcripts were differentially expressed with statistical significance ($p \leq 0.05$, and $|FC| \geq 1.0$) in the NP-impaired and the recovered cells, respectively. The functional groups of the differentially regulated genes were generally categorized into the groups of cellular membrane metabolism or transport, information processing, amino acid or carbohydrate metabolism, energy production or conversion, cellular defense or repair, and secondary metabolisms (Fig. S3). Except for the unknown genes, the three most significantly expressed functional genes in the NP-impaired cells were related to amino acid metabolism, membrane biogenesis, and RNA translation or ribosomal metabolism. In addition, the number of differentially expressed genes in the clustered functional groups generally decreased after 40-d NP stress (Fig. S3). Overall, the transcriptional expression patterns of the NP-impaired cells after their 12-d and 40-d exposure to NPs were comparable and the NP toxicity impacts on the cells' transcriptional expressions were generally alleviated by the extension of the NP exposure time.

3.3.1 Amino acid and RNA translation or ribosomal metabolisms

Nineteen of the 22 amino acid metabolism-related genes encoding transferase, synthase, reductase, isomerase, and kinase were significantly up-regulated after 12-d NP stress, whereas only 3 genes encoding methionine and arginine metabolism were down-regulated (Fig. 4A). However,

the over-expression levels of these genes were generally alleviated after 40-d incubation and 18 of the 22 affected genes reverted back to their original expression levels. These results strongly suggested that the regulations of amino acid metabolism at the transcriptional level actively participated in the cellular adaption and recovery processes under TiO_2 NP stress.

Nineteen transcripts encoding RNA translation or ribosomal metabolism were dramatically up-regulated after 12-d and 40-d NP impacts (Fig. 4B). With prolonged NP impact, 13 of the 19 up-regulated genes reverted back to the original levels. In contrast, 12 transcripts encoding RNA helicase, methyltransferase, and 16/30S ribosomal protein were over-expressed only after 40-d NP exposure. Overall, the self-regulations of the aminoacyl-tRNA biosynthesis, RNA translation, and the ribosomal metabolism pathways in the TiO_2 NP-impaired cells were probably significantly activated to resist the NP stress.

3.3.2 Membrane transport and associated metabolisms

The NPs interrupted the expression of the membrane transport and biogenesis-related genes encoding inorganic ion transporters, membrane efflux, membrane fusion, and peptidoglycan biosynthesis (Fig. 5). After 12-d NP exposure, 19 genes mainly encoding transmembrane binding, receptor, fusion, or efflux proteins for general substrate transport and acriflavin resistance were significantly up-regulated ($p \leq 0.05$, $FC \geq 1$). The 18 genes that were significantly down-regulated ($p \leq 0.05$, $FC \leq -1$) were mainly related to sulfate, copper, or ammonium transport and glycometabolism. However, 22 of these up/down-regulated transcripts were able to return to their original expression levels after 40-d incubation, which indicated the possible membrane repair regulations. In addition, transcripts encoding acriflavin resistance, major facilitator transport, or pore ion channels were further up-regulated and 6 transcripts encoding peptidoglycan biosynthesis were down-regulated after 40-d NP exposure. Therefore, the membrane metabolism associated regulations were actively involved in cellular adaption/recovery during the chronic NP exposure.

3.3.3 Energy metabolisms

Thirteen and 5 transcripts for energy production/conversion were statistically differentially

expressed ($p \leq 0.05$, $|FC| > 1$) after 12-d and 40-d NP stress, respectively (Fig. 6). Among them, 4 genes involved with the respiratory chain or electron transport and ATP production were up-regulated during the entire incubation period. The down-regulated transcripts were mainly related to NADH-quinone reduction and the tricarboxylic acid (TCA) cycle. After 40-d incubation, the expressions of up-regulated genes were significantly lessened except for one ATP-citrate lyase-encoding gene and all the significantly down-regulated transcripts regained their original expression levels. Therefore, the energy production/conversions pathways were probably impacted by the TiO_2 NPs and the associated regulations of the respiration chain and ATP production were assumed to be actively involved in the cellular adaption and recovery processes.

3.4 Verification of microarray results

Three representative genes at different expression levels were subjected to qRT-PCR for verification of the microarray results. The gene NE0669 encoding the acriflavin resistance protein for stress resistance was highly up-regulated with an FC of 4.30 and 4.99 after 12-d and 40-d NP stress, respectively (Table 1). The gene *Rh50* encoding ammonium transporters and the gene NE0371 encoding the TonB-dependent receptor protein were both significantly differentially expressed (Table 1). Generally, their expressions as quantified by the qRT-PCR displayed similar varying trends as the microarray results although a smaller FC ratio was obtained with the qRT-PCR.

4 Discussion

4.1 Cell responses and adaptions to long-term TiO_2 NP exposure

N. europaea displayed a strong adaptation potential during the long-term exposure to TiO_2 NPs in a continuous cultivation reactor and the compromised cell density, membrane integrity, nitritation performance, and AMO activity gradually recovered (Fig. 1-3). The nitritation performances of AOB were observed to recover from 0.1 mg/L Ag NPs stress in a nitrifying SBR (Alito and Gunsch 2014) and 150-d ZnO NP exposure in a completely autotrophic nitrogen removal over nitrite

(CANON) system (Zhang et al. 2017). These results reflect the possible anti-toxicity and adaptation capacities of AOB under NP stress. It was assumed that the diversity of the microbial community and the survival of insensitive bacteria contributed to the recovery of the BNR performances as a result of a selection process under Ag NP (Alito and Gunsch 2014) and ZnO NP stress (Zhang et al. 2017). Considering the different sensitivity of *N. europaea* cells during their 8-12 h generation time (Skinner and Walker 1961), the cell density first decreased and then recovered (Fig. 1A); this may be attributable to the sensitive cells' decay and the continuous cell proliferation. However, the membrane integrity improvement (Fig. 1B) and structure distortion alleviation (Fig. 2) indicated that the response of *N. europaea* to the TiO_2 NPs might not only be attributed to selection but may also be an 'inhibition-recovery' process. The 50 mg/L ZnO NP-impacted continuously grown *N. europaea* cells have been reported to revert to their metabolic performances after the release of 6-h NP stress although the prolonging of the ZnO NP impacts finally caused irreversible cell impairment (Wu et al. 2017). TiO_2 NPs are generally photosensitive and cause photooxidative damage to cells (Miller et al. 2012). In this study, the cells were exposed to TiO_2 NPs in the dark and the NPs' non-photooxidative stress and physical 'stab' (Liu et al. 2009) probably contributed to the main nanotoxicity effects. ZnO NPs with high solubility are well known to cause more toxic impacts than TiO_2 NPs (Yu et al. 2015). Therefore, the impaired cells were expected to display greater adaption or recovery potentials under less toxic TiO_2 stress than ZnO NPs.

4.2 RNA translation or ribosomal metabolism regulations

The stimulation of RNA translation or ribosomal metabolism pathways, such as aminoacyl-tRNA biosynthesis and RNA or ribosome modifications, are probably involved in mediating functional protein or enzyme synthesis as cellular anti-toxicity and self-adaption behaviors. It is well known that aminoacyl-tRNA synthetase catalyzes the primary step of the protein biosynthesis via attaching amino acids to the associated tRNAs (Schimmel and Söll 1979). Aminoacyl-tRNA synthetases including glycine, arginine, and leucine were demonstrated to be positively correlated with the *Escherichia coli* growth rate (Neidhardt et al. 1977). The observed

up-regulation of aminoacyl-tRNA (*gatAB*) and the associated amino acid (*gcvTH1*, *argC*, and *leuA*) biosynthesis encoding genes in response to the 12-d TiO_2 NP stress (Fig. 4) probably promoted the cell growth to regain the original cell density (Fig. 1A). The up-regulations of *gatAB* and the amino acid encoding genes *argB* and *hisD* for energy conservation were reported to resist 1 μM cadmium stress (Park and Ely 2008a), which further supported the findings that RNA translations and the associated amino acid biosynthesis pathways were stimulated for cellular resistance and adaption to the TiO_2 NP stress. Ribosomes are considered the main sites for cellular protein biosynthesis (Ramakrishnan 2002). The increased expressions of the ribosomal protein biogenesis encoding operators, such as *rpsDE*, *rpmF*, and *rplQ* were detected in the *N. europaea* cells in response to zinc, linear alkylbenzene sulfonates, or ZnO NPs stress to resist toxicity effects (Wu et al. 2017; Urakawa et al. 2008; Park and Ely 2008b). Thus, the observed up-regulation of the ribosome biosynthesis (*rpsBU*) or the modification factor (*truB, ksgA*) encoding genes (Fig. 4) might contribute to the recovery of the impaired protein or enzyme functions and the improvement in the metabolic activities. Overall, the stimulations of the RNA translation or ribosomal metabolism regulations promoted the resistance and recovery process of *N. europaea* to the TiO_2 NP stress.

4.3 Membrane metabolism regulations

Membrane repair involved transport and the associated metabolism regulation processes are crucial for the cells' adaption to the TiO_2 NP stress. Fang et al. (2007) reported on the variations of the membrane lipid components and membrane fluidity in denitrification-associated *Bacillus subtilis* to resist fullerene NP stress. In our study, the NP-impaired membrane integrity gradually increased with the increase in the NP exposure time (Fig. 1B), which suggested the possible membrane repair processes. Our microarray results further revealed the varied expressions of numerous transcripts encoding the membrane transport, efflux system, and structure preservation during the chronic TiO_2 NP stress (Fig. 5). For example, the expressions of acriflavin resistance (NE0669), the membrane efflux/fusion protein (NE0373, NE0668, NE0670), and the major facilitator transporter (MFC) (NE2454) genes were up-regulated. These genes are associated with

efflux pumps (EP) (Chain et al. 2003) for drug-resistance or environmental stress-resistance regulations (Amaral et al. 2011), which are generally performed by a combination of an inner efflux protein and a membrane-embedded fusion protein (Ma et al. 1994). The up-regulation of the EP-associated genes might be a survival or adaption effort of the NP-impaired cells trying to capture the potential 'invaders' and transport them outside the membrane for toxin exclusion and stress alleviation. The EP-associated genes were also found to be overexpressed due to stress resistance or alleviation in response to heavy metals (Park and Ely 2008a) and ZnO NP (Wu et al. 2017) stress. In addition, magnesium is essential for cell growth as a cofactor during ATP-requiring enzymatic catalysis and plays a critical role in transmembrane electrolyte flux adjustment via binding the active site or causing a conformational change of the enzyme (Ryan 1991). An increase in the magnesium concentration from 270 to 2,250 μM was reported to promote the nitrifying activity of *N. europaea* under Zn^{2+} stress (Radniecki et al. 2009). Therefore, the observed up-regulation of the magnesium transporter-associated gene (NE0373) indicated cellular self-protection/recovery behavior to help recover the impaired membrane permeability and nitrifying activities under NP stress. Furthermore, potassium is known as an osmotic solute to activate enzymes or transport systems for cellular osmotic-regulation (Epstein 2003). The transmembrane potential is mainly determined by the transmembrane potassium gradient (Corratgé-Faillie et al. 2010). The NP damaged cell membrane integrity (Fig. 1B) and structure (Fig. 2B) might lead to a potassium leakage outside the membrane, thus disrupting the transmembrane potential and osmotic balance. The observed up-regulation of the potassium transporter-encoding gene (*trkA*) suggested that the cells' active potassium transport processes probably prevent an inner potassium deficiency and maintain the transmembrane osmotic balance to resists the TiO_2 NP stress.

At the end of the 40-d NP stress, the regulated transcript expressions encoding the membrane-related metabolisms were generally alleviated (Fig. 5), which indicated the cell's physiological performance recovery potentials (Fig. 1-3). For instance, the inhibited expressions of the genes encoding the sulfate (*cysAW*) and ammonium transport (*Rh50*) recovered and returned

back to their original levels after 12-d TiO_2 stress. The decreased expressions of the cyanophycin synthetase encoding genes (NE0922/0923) for substrate reservation (Hai et al. 2006) significantly recovered during the chronic TiO_2 NP stress. It is noteworthy that the expression of the genes encoding the peptidoglycan biosynthesis (Fig. 5), an important membrane constituent for skeleton structure preservation (Vollmer et al. 2008, Vollmer and Höltje 2004) were continuously depressed in accordance with the impaired cell membrane structure (Fig. 2C); this was probably due to the persistent NP-cell contact that compromised the cell membrane mending effects. In summary, the interruptions of the membrane structure and the associated functions represented the important toxicity mechanisms of the TiO_2 NPs and the regulations of the corresponding membrane-related metabolic processes were crucial for the cells' self-adaption and recovery processes.

4.4 Energy metabolism regulations

The regulations of the energy metabolisms, such as the respiratory electron transfer chain and the TCA cycle pathways contributed to the cells' adaption to the TiO_2 NP stress. After 12-d exposure to the NPs, the cytochrome c oxidase (*SCO1*, NE0926) and ATP production (*atpB*) encoding transcripts (Fig. 6) were stimulated although the NADH-ubiquinone oxidoreductase encoding genes (*nqrBCD*) for NADH consumption (EC 1.6.5.8) were down-regulated. The cells probably recovered the energy production efficiency by promoting the electron transfer and ATP production via stimulation of the proton gradient generation in the electron transfer chain (Chain et al. 2003). In addition, the significantly inhibited energy-associated gene expressions generally reverted back to their original level ($|FC| < 1$) with the increase in the cell incubation time under the NP stress, especially for the TCA cycle-related encoding transcripts (*sucB, sdhAD*) responsible for the recovery of respiration and the TCA cycle-related energy metabolisms. Moreover, the continuous up-regulations of the genes *coxBA2* related to the oxygen-dependent proton gradient generations (Keilin and Hartree 1938) and *atpB* involved in ATP production (Kumar and Nicholas 1982) might further enhance the energy production efficiency during the prolonged NP exposure period; this behavior has been observed in *N. europaea* cells after 6-h exposure to 50 mg/L ZnO

NPs as a self-resistance response (Wu et al. 2017). Overall, the energy metabolism pathways including the respiratory electron transfer and the TCA cycle were impacted by the TiO_2 NPs and the stimulations of the oxygen-dependent electron transfer and the proton-dependent ATP production were assumed to increase the cellular energy production/conversion for cell adaption to the TiO_2 NP chronic stress.

4.5 Toxin-antitoxin, non-photooxidative stress responses and DNA repair

The toxin-antitoxin (TA) system is generally considered to be involved in the prokaryotic defense and stress-related adaptation (Van Melderen 2010). Two type II TA genes (NE1563, NE1583) and one TA system-related gene (*mreB*) were up-regulated after 12-d and 40-d NP stress, respectively (Table 2). The over-expressions of the TA genes might contribute to the cellular adaption to the TiO_2 NP stress and this may occur via genomic fragment stabilization and DNA protection (Wozniak and Waldor 2009). The up-regulation of the DNA repair and replication encoding genes (e.g. *rdgC* and *ssb*, Table 2) further supported the cells' TA adaption mechanism. Some studies have reported the regulation of TA genes in *N. europaea* cells when threatened by chloroform and ZnO NPs (Wu et al. 2017, Gvakharia et al. 2007). In addition, the up-regulation of the oxidative stress response-related genes were also detected even in the dark (Table 2). TiO_2 has been demonstrated to induce ROS generation and exert oxidative damage on biofilm microbes (Battin et al. 2009) and human cells (Sayes et al. 2006) in the absence of light. The extracytoplasmic function (ECF) sigma factor is considered to be involved in 'stress-fighting' as an oxidative stress response (Chain et al. 2003). Thioredoxin with reducing ability is also widely recognized as a detoxicant for oxidative stress alleviation under NP stress (Yang et al. 2012). The observed up-regulation of these stress-defense related genes indicated their contributions to cellular adaptions under chronic TiO_2 NP stress.

4.6 DO impact on cellular adaption

The cells cultured under either 0.5 or 2.0 mg/L DO conditions regained the previously decreased cell density, membrane integrity, nitritation performance, and AMO activity at the end of

the 40-d incubation with TiO_2 NPs. Nevertheless, the low-DO cultivated cells were more susceptible to the TiO_2 NPs stress and required more time for adaption (Fig. 1 & 3). *N. europaea* cells are well known to obtain energy from ammonia oxidation by using only two of four produced electrons from hydroxylamine oxidation for ATP production (Prosser 1990), which results in a low net gain in terms of energy production/conversion. When the oxygen supply was low, the proton-driven force generated by the oxygen reduction for the ATP production was inefficient, which might cause the severe limitation of the energy conversion and the associated substance metabolism, such as the carbon fixation, the TCA cycle, the amino acid metabolism, and the membrane metabolism (Chain et al. 2003). In addition, the electron transfer chain originating from the NH_2OH oxidation might be stimulated to enhance the energy production efficiency for stress resistance and adaption because the cytochrome c oxidase encoding genes were significantly up-regulated after NP exposure (Fig. 6), whereas the cycled electron transfer chain back to the AMO catalyzation was inhibited (Fig. S4), which resulted in the inhibition of the AMO activity (Fig. 3C). Whittaker et al. (2000) have also reported similar energy regulation and AMO inhibition mechanisms under protonophore chlorocarbonylcyanidephenyl hydrazone (CCCP) stress. Therefore, under lower DO levels, the stimulation of energy production by oxygen reduction for cell resistance/adaption might be insufficient, which might cause more severe AMO limitations (Fig. 3C). Furthermore, the up-regulation of the gene *coxBA2* encoding cytochrome oxidase aa3 for the oxygen-dependent proton gradient generation (Keilin and Hartree 1938) and the stimulation of the ATP production were responsible for the cellular adaptions as discussed above, which might be potentially depressed under low DO conditions (Fig. S4). Overall, an insufficient oxygen supply might exert negative effects on the stimulation of energy production/conversion and the regulations of the related metabolisms and finally result in lower cell adaption potentials at low DO conditions.

5 Conclusion

The novelty of this study was a comprehensive exploration of the adaption and recovery of an

ammonia oxidizer, *N. europaea,* under chronic TiO_2 NP stress and different DO conditions at the physiological, metabolic, and transcriptional levels. A deep understanding of the self-adaptive regulations or self-recovery potentials of NP-impaired AOB is essential and crucial for developing emergency adjustment strategies in response to NP contamination in the BNR process. The main findings of this study are:

- The impaired cell density, membrane integrity, nitritation performance, and specific AMO activity recovered after exposure to 50 mg/L TiO_2 NP long-term stress.
- Low DO cultivated cells were more susceptible to chronic NP stress and displayed less efficient adaption capacities; this was probably due to the limitation of the oxygen-dependent energy production/conversion with a deficient oxygen supply.
- The interruption of the membrane structure and the associated functions were the direct consequences of the biotoxicity of the TiO_2 NPs. The corresponding regulations of the membrane-associated metabolic processes were crucial for the cellular self-adaption and recovery processes, such as the membrane efflux for toxicants exclusion, maintenance of the structural stability, membrane osmotic adjustment, and substrate transport regulation.
- The stimulations of the RNA translation or ribosomal metabolisms including the aminoacyl-tRNA biosynthesis and RNA /ribosome modification pathways were actively involved in cell growth promotion and cellular adaptions to the NP stress.
- The regulations of the energy metabolisms, especially the TCA cycle, the electron transfer, and the ATP biosynthesis pathways enhanced the energy production efficiency for cell recovery.
- TA ‘stress fighting’, non-photooxidative stress quenching, and DNA repair processes were also actively involved in the cellular adaption and recovery during the long-term exposure to the TiO_2 NPs stress.

Acknowledgment

This work was supported by National Natural Science Foundation of China (51678134 and 51208092), Natural Science Foundation of Jiangsu Province, China (SBK2017020636), Innovative Graduate Student Project of Jiangsu Province (KYLX16_0282), and Scientific Research Foundation of Graduate School of Southeast University. The authors thank Alejandro Palomo from Technical University of Denmark for the helpful comments on the manuscript.

References

Alito, C.L. and Gunsch, C.K. (2014) Assessing the effects of silver nanoparticles on biological nutrient removal in bench-scale activated sludge sequencing batch reactors. Environmental Science and Technology 48(2), 970-976.

Amaral, L., Fanning, S. and Pagès, J.-M. (2011) Advances in Enzymology and Related Areas of Molecular Biology. Toone, E.J. (ed).

Battin, T.J., Kammer, F.v.d., Weilhartner, A., Ottofuelling, S. and Hofmann, T. (2009) Nanostructured TiO_2: Transport behavior and effects on aquatic microbial communities under environmental conditions. Environmental Science and Technology 43(21), 8098-8104.

Binh, C.T.T., Adams, E., Vigen, E., Tong, T., Alsina, M.A., Gaillard, J.-F., Gray, K.A., Peterson, C.G. and Kelly, J.J. (2016) Chronic addition of a common engineered nanomaterial alters biomass, activity and composition of stream biofilm communities. Environmental Science: Nano 3(3), 619-630.

Chain, P., Lamerdin, J., Larimer, F., Regala, W., Lao, V., Land, M., Hauser, L., Hooper, A., Klotz, M., Norton, J., Sayavedra-Soto, L., Arciero, D., Hommes, N., Whittaker, M. and Arp, D. (2003) Complete genome sequence of the ammonia-oxidizing bacterium and obligate chemolithoautotroph *Nitrosomonas europaea*. Journal of Bacteriology 185(9), 2759-2773.

Corratgé-Faillie, C., Jabnoune, M., Zimmermann, S., Véry, A.-A., Fizames, C. and Sentenac, H. (2010) Potassium and sodium transport in non-animal cells: the Trk/Ktr/HKT transporter

family. Cellular and Molecular Life Sciences 67(15), 2511-2532.

Epstein, W. (2003) The roles and regulation of potassium in bacteria. Progress in Nucleic Acid Research and Molecular Biology 75, 293-320.

Fang, J.S., Lyon, D.Y., Wiesner, M.R., Dong, J.P. and Alvarez, P.J.J. (2007) Effect of a fullerene water suspension on bacterial phospholipids and membrane phase behavior. Environmental Science and Technology 41(7), 2636-2642.

Gondikas, A.P., Von Der Kammer, F., Reed, R.B., Wagner, S., Ranville, J.F. and Hofmann, T. (2014) Release of TiO_2 nanoparticles from sunscreens into surface waters: a one-year survey at the Old Danube recreational lake. Environmental Science and Technology 48(10), 5415–5422.

Gottschalk, F., Sonderer, T., Scholz, R.W. and Nowack, B. (2009) Modeled environmental concentrations of engineered nanomaterials (TiO_2, ZnO, Ag, CNT, Fullerenes) for different regions. Environmental Science and Technology 43(24), 9216-9222.

Gvakharia, B., Permina, E., Gelfand, M., Bottomley, P., Sayavedra-Soto, L. and Arp, D. (2007) Global transcriptional response of *Nitrosomonas europaea* to chloroform and chloromethane. Applied and Environmental Microbiology 73(10), 3440-3445.

Hai, T., Frey, K.M. and Steinbuchel, A. (2006) Engineered cyanophycin synthetase (*CphA*) from Nostoc ellipsosporum confers enhanced *CphA* activity and cyanophycin accumulation to Escherichia coli. Applied and Environmental Microbiology 72(12), 7652-7660.

Hu, Q., Guo, F., Zhao, F. and Fu, Z. (2017) Effects of titanium dioxide nanoparticles exposure on parkinsonism in zebrafish larvae and PC12. Chemosphere 173, 373-379.

Huang, G., Ng, T.W., An, T., Li, G., Wang, B., Wu, D., Yip, H.Y., Zhao, H. and Wong, P.K. (2017) Interaction between bacterial cell membranes and nano-TiO_2 revealed by two-dimensional FTIR correlation spectroscopy using bacterial ghost as a model cell envelope. Water Research 118, 104-113.

Keilin, D. and Hartree, E.F. (1938) Cytochrome *a* and cytochrome oxidase. Nature 141, 870-871.

Kowalchuk, G.A. and Stephen, J.R. (2001) Ammonia-oxidizing bacteria: a model for molecular microbial ecology. Annual Review of Microbiology 55, 485-529.

Kumar, S. and Nicholas, D.J.D. (1982) A protonmotive force-dependent adenosine-5′ triphosphate synthesis in spheroplasts of *Nitrosomonas europaea*. FEMS Microbiology Letters 14, 21-25.

Li, B., Huang, W., Zhang, C., Feng, S., Zhang, Z., Lei, Z. and Sugiura, N. (2015) Effect of TiO_2 nanoparticles on aerobic granulation of algal–bacterial symbiosis system and nutrients removal from synthetic wastewater. Bioresource Technology 187, 214-220.

Li, D., Li, B., Wang, Q., Hou, N., Li, C. and Cheng, X. (2016) Toxicity of TiO_2 nanoparticle to denitrifying strain CFY1 and the impact on microbial community structures in activated sludge. Chemosphere 144, 1334-1341.

Li, Y., Zhang, W., Niu, J.F. and Chen, Y.S. (2012) Mechanism of photogenerated reactive oxygen species and correlation with the antibacterial properties of engineered metal-oxide nanoparticles. ACS Nano 6(6), 5164-5173.

Li, Z., Wang, X., Ma, B., Wang, S., Zheng, D., She, Z., Guo, L., Zhao, Y., Xu, Q., Jin, C., Li, S. and Gao, M. (2017) Long-term impacts of titanium dioxide nanoparticles (TiO_2 NPs) on performance and microbial community of activated sludge. Bioresource Technology 238, 361-368.

Liu, S.B., Wei, L., Hao, L., Fang, N., Chang, M.W., Xu, R., Yang, Y.H. and Chen, Y. (2009) Sharper and faster "Nano Darts" kill more bacteria: A study of antibacterial activity of individually dispersed pristine single-walled carbon nanotube. ACS Nano 3(12), 3891-3902.

Liu, W., Bertrand, M., Chaneac, C. and Achouak, W. (2016) TiO_2 nanoparticles alter iron homeostasis in *Pseudomonas brassicacearum* as revealed by PrrF sRNA modulation. Environmental Science Nano 3, 1473–1482.

Ma, D., Cook, D.N., Hearst, J.E. and Nikaido, H. (1994) Efflux pumps and drug resistance in gram-negative bacteria. Trends in Microbiology 2(12), 489-493.

Miller, R.J., Bennett, S., Keller, A.A., Pease, S. and Lenihan, H.S. (2012) TiO_2 nanoparticles are phototoxic to marine phytoplankton. PloS One 7(1), e30321.

Minetto, D., Libralato, G. and Volpi Ghirardini, A. (2014) Ecotoxicity of engineered TiO_2 nanoparticles to saltwater organisms: An overview. Environment International 66, 18-27.

Neidhardt, F.C., Bloch, P.L., Pedersen, S. and Reeh, S. (1977) Chemical measurement of steady-state levels of ten aminoacyl-transfer ribonucleic acid synthetases in *Escherichia coli*. Journal of Bacteriology 129(1), 378-387.

Park, S. and Ely, R.L. (2008a) Candidate stress genes of *Nitrosomonas europaea* for monitoring inhibition of nitrification by heavy metals. Applied and Environmental Microbiology 74(17), 5475-5482.

Park, S. and Ely, R.L. (2008b) Genome-wide transcriptional responses of *Nitrosomonas europaea* to zinc. Archives of Microbiology 189(6), 541-548.

Piccinno, F., Gottschalk, F., Seeger, S. and Nowack, B. (2012) Industrial production quantities and uses of ten engineered nanomaterials in Europe and the world. Journal of Nanoparticle Research 14(9), 1109.

Polesel, F., Farkas, J., Kjos, M., Almeida Carvalho, P., Flores-Alsina, X., Gernaey, K.V., Hansen, S.F., Plósz, B.G. and Booth, A.M. (2018) Occurrence, characterisation and fate of (nano)particulate Ti and Ag in two Norwegian wastewater treatment plants. Water Research 141, 19-31.

Prosser, J.I. (1990) Autotrophic nitrification in bacteria. Advances in Microbial Physiology 30, 125-181.

Radniecki, T.S., Semprini, L. and Dolan, M.E. (2009) Expression of *merA*, *amoA* and *hao* in continuously cultured *Nitrosomonas europaea* cells exposed to zinc chloride additions. Biotechnology and Bioengineering 102(2), 546-553.

Ramakrishnan, V. (2002) Ribosome structure and the mechanism of translation. Cell 108(4), 557-572.

599 Robichaud, C.O., Uyar, A.E., Darby, M.R., Zucker, L.G. and Wiesner, M.R. (2009) Estimates of
600 upper bounds and trends in nano-TiO_2 production as a basis for exposure assessment.
601 Environmental Science and Technology 43(12), 4227-4233.
602 Ryan, M.F. (1991) The role of magnesium in clinical biochemistry: An overview. Annals of
603 Clinical Biochemistry 28(1), 19-26.
604 Schimmel, P.R. and Söll, D. (1979) Aminoacyl-tRNA synthetases: general features and recognition
605 of transfer RNAs. Annual Review of Biochemistry 48, 601-648.
606 Sayes, C.M., Wahi, R., Kurian, P.A., Liu, Y., West, J.L., Ausman, K.D., Warheit, D.B. and Colvin,
607 V.L. (2006) Correlating nanoscale titania structure with toxicity: A cytotoxicity and
608 inflammatory response study with human dermal fibroblasts and human lung epithelial cells.
609 Toxicological Sciences 92(1), 174-185.
610 SEPAC (2002) Methods for monitor and analysis of water and wastewater China Environment
611 Science Press (in Chinese), Beijing.
612 Skinner, F.A. and Walker, N. (1961) Growth of *Nitrosomonas europaea* in batch and continuous
613 culture. Archives of Microbiology 38(4), 339-349.
614 Sun, T.Y., Gottschalk, F., Hungerbuhler, K. and Nowack, B. (2014) Comprehensive probabilistic
615 modelling of environmental emissions of engineered nanomaterials. Environmental
616 Pollution 185, 69-76.
617 Urakawa, H., Matsumoto, J., Inaba, K. and Tsuneda, S. (2008) DNA microarray mediated
618 transcriptional profiling of *Nitrosomonas europaea* in response to linear alkylbenzene
619 sulfonates. FEMS Microbiology Letters 282(2), 166-173.
620 Van Melderen, L. (2010) Toxin–antitoxin systems: why so many, what for? Current Opinion in
621 Microbiology 13(6), 781-785.
622 Vance, M.E., Kuiken, T., Vejerano, E.P., Mcginnis, S.P., Jr, H.M., Rejeski, D. and Hull, M.S.
623 (2015) Nanotechnology in the real world: Redeveloping the nanomaterial consumer
624 products inventory. Beilstein Journal of Nanotechnology 6, 1769-1780.

Vollmer, W., Blanot, D. and De Pedro, M. (2008) Peptidoglycan structure and architecture. FEMS Microbiology Reviews 32(2), 149–167.

Vollmer, W. and Höltje, J.-V. (2004) The architecture of the murein (peptidoglycan) in gram-negative bacteria: Vertical scaffold or horizontal layer(s)? Journal of Bacteriology 186(18), 5978-5987.

Westerhoff, P., Song, G.X., Hristovski, K. and Kiser, M.A. (2011) Occurrence and removal of titanium at full scale wastewater treatment plants: implications for TiO_2 nanomaterials. Journal of Environmental Monitoring 13(5), 1195-1203.

Whittaker, M., Bergmann, D., Arciero, D. and Hooper, A.B. (2000) Electron transfer during the oxidation of ammonia by the chemolithotrophic bacterium Nitrosomonas europaea. Biochimica et Biophysica Acta 1459(2-3), 346-355.

Wozniak, R.A.F. and Waldor, M.K. (2009) A toxin–antitoxin system promotes the maintenance of an integrative conjugative element. PLoS Genetics 5(3), e1000439.

Wu, J., Lu, H., Zhu, G., Chen, L., Chang, Y. and Yu, R. (2017) Regulation of membrane fixation and energy production/conversion for adaptation and recovery of ZnO nanoparticle impacted *Nitrosomonas europaea*. Applied Microbiology and Biotechnology 101(7), 2953-2965.

Yang, Y., Wang, J., Xiu, Z. and Alvarez P.J. (2013) Impacts of silver nanoparticles on cellular and transcriptional activity of nitrogen□cycling bacteria. Environmental Toxicology and Chemistry 32(7), 1488-1494.

Yang, Y., Wang, J., Zhu, H., Colvin, V.L. and Alvarez, P.J. (2012) Relative susceptibility and transcriptional response of nitrogen cycling bacteria to quantum dots. Environmental Science and Technology 46(6), 3433-3441.

Yu, Q., Wang, H., Peng, Q., Li, Y., Liu, Z. and Li, M. (2017) Different toxicity of anatase and rutile TiO_2 nanoparticles on macrophages: Involvement of difference in affinity to proteins and phospholipids. Journal of Hazardous Materials 335, 125-134.

651 Yu, R., Fang, X., Somasundaran, P. and Chandran, K. (2015) Short-term effects of TiO_2, CeO_2, and
652 ZnO nanoparticles on metabolic activities and gene expression of *Nitrosomonas europaea*.
653 Chemosphere 128, 207-215.
654 Yu, R., Wu, J., Liu, M., Zhu, G., Chen, L., Chang, Y. and Lu, H. (2016) Toxicity of binary mixtures
655 of metal oxide nanoparticles to *Nitrosomonas europaea*. Chemosphere 153, 187-197.
656 Zahra, Z., Waseem, N., Zahra, R., Lee, H., Badshah, M.A., Mehmood, A., Choi, H.-K. and Arshad,
657 M. (2017) Growth and metabolic responses of rice (*Oryza sativa L.*) cultivated in
658 phosphorus deficient soil amended with TiO_2 nanoparticles. Journal of Agricultural and
659 Food Chemistry 65(28), 5598–5606.
660 Zhang, X., Zhang, N., Fu, H., Chen, T., Liu, S., Zheng, S. and Zhang, J. (2017) Effect of zinc oxide
661 nanoparticles on nitrogen removal, microbial activity and microbial community of CANON
662 process in a membrane bioreactor. Bioresource Technology 243, 93-99.
663 Zhang, X., Zhou, Y., Xu, T., Zheng, K., Zhang, R., Peng, Z. and Zhang, H. (2018) Toxic effects of
664 CuO, ZnO and TiO_2 nanoparticles in environmental concentration on the nitrogen removal,
665 microbial activity and community of anammox process. Chemical Engineering Journal 332,
666 42-48.
667 Zheng, X., Chen, Y. and Wu, R. (2011a) Long-term effects of titanium dioxide nanoparticles on
668 nitrogen and phosphorus removal from wastewater and bacterial community shift in
669 activated sludge. Environmental Science and Technology 45(17), 7284-7290.
670 Zheng, X.O., Wu, R. and Chen, Y.G. (2011b) Effects of ZnO nanoparticles on wastewater
671 biological nitrogen and phosphorus removal. Environmental Science and Technology 45(7),
672 2826-2832.
673 Zhou, X.H., Huang, B.C., Zhou, T., Liu, Y.C. and Shi, H.C. (2015) Aggregation behavior of
674 engineered nanoparticles and their impact on activated sludge in wastewater treatment.
675 Chemosphere 119, 568-576.
676

Figure Captions

Fig. 1 Changes in the cell concentration (A) and membrane integrity (B) under different DO conditions during chronic TiO_2 NP exposure

Fig. 2 TEM images of normal cells (A), 12-d (B), and 40-d (C) TiO_2 NP-impaired cells with a DO concentration of 2.0 mg/L. The red arrows indicate the distortion of the membrane and the yellow arrows indicate the undistinguishable membrane structure.

Fig. 3 Changes in the ammonium (A) and nitrite (B) concentrations and the specific AMO activities (C) in the chemostat reactor at different DO concentrations under chronic TiO_2 NP exposure

Fig. 4 Heat map images of the functional gene expressions related to amino acid (A) and RNA translation or ribosomal (B) metabolisms in the pre-exposure cells, 12-d, and 40-d TiO_2 NP-impaired cells. ('*' indicates no statistical differences between the gene expressions compared to the pre-exposure cells, $p > 0.05$ or $|FC| < 1.0$)

Fig. 5 Differentially expressed functional genes related to inorganic ion transport and metabolism and cell membrane biogenesis after 12-d and 40-d exposure to 50 mg/L TiO_2 NPs; the pre-exposure cells are the reference ($p \leq 0.05$, $|FC| \geq 1.0$).

Fig. 6 Differentially expressed functional genes encoding for energy production/conversion after 12-d and 40-d exposure to 50 mg/L TiO_2 NPs; the pre-exposure cells are the reference ($p \leq 0.05$, $|FC| \geq 1.0$).

Table 1 Microarray and qRT-PCR analysis of selected functional genes after 12-d and 40-d exposure to 50 mg/L TiO_2 NPs, respectively; the pre-exposure cells are the reference.

Locus tag	Gene	Product	Sample	Microarray fold-change (log_2 value)	*p*-value	qRT-PCR fold-change (log_2 value)
Down-regulation						
NE0448	*Rh50*	Ammonium transporter	12-d	-2.46	1.51×10^{-3}	-2.34[a]
			40-d	-1.74	7.20×10^{-3}	-0.85
Up-regulation						
NE0669		Acriflavin resistance protein	12-d	4.30	2.09×10^{-5}	2.31[a]
			40-d	4.99	5.47×10^{-7}	2.01[a]
NE0731		TonB-dependent receptor protein	12-d	1.07	2.23×10^{-2}	0.86
			40-d	2.58	6.22×10^{-4}	1.41[a]

[a] indicates statistically significant with *p*–value ≤ 0.05.

Table 2 Selected functional genes with significant transcriptional responses to 50 mg/L TiO_2 NPs (|FC| ≥ 1, $p \leq 0.05$).

Gene	Locus_ tag	Product	Description	FC (log_2 value)	
				Imp./Pre.	Rec./Pre.
Toxin-antitoxin genes					
	NE1563	Hypothetical protein	Type II TA system, RelE/StbE-RelB/StbD	1.17	-
	NE1584	Hypothetical protein	Type II TA system, RelE/StbE-RelB/StbD	1.04	-
mreB	NE2070	Rod shape-determining protein MreB	Type II TA system-related factors	-	1.88
ECF subfamily genes					
	NE0547	ECF subfamily RNA polymerase sigma factor	Transcription machinery, oxidative stress response	1.05	-
	NE1041	ECF subfamily RNA polymerase sigma-70 factor	Transcription machinery, oxidative stress response	1.08	1.05
	NE1992	ECF subfamily RNA polymerase sigma factor	Transcription machinery, oxidative stress response	1.02	-
	NE1001	ECF subfamily RNA polymerase sigma factor	Transcription machinery, oxidative stress response	-	1.06
Thioredoxin gene					
	NE1319	Thioredoxin	Oxidative stress response	1.26	-
DNA repair/replication genes					
rdgC	NE0507	Recombination associated protein	DNA repair, double-strand breaks repair	1.48	1.01
ssb	NE2453	Single-strand binding protein family	DNA repair, single-strand breaks repair	1.37	2.12
	NE0098	DnaA regulatory inactivator Hda	DNA replication	1.02	-
	NE0001	Chromosomal replication initiation protein	DNA replication, initiation factors	-	1.50
	NE1850	ATP-dependent DNA helicase RecG	DNA repair, double-strand breaks repair	-	1.01

Fig. 1

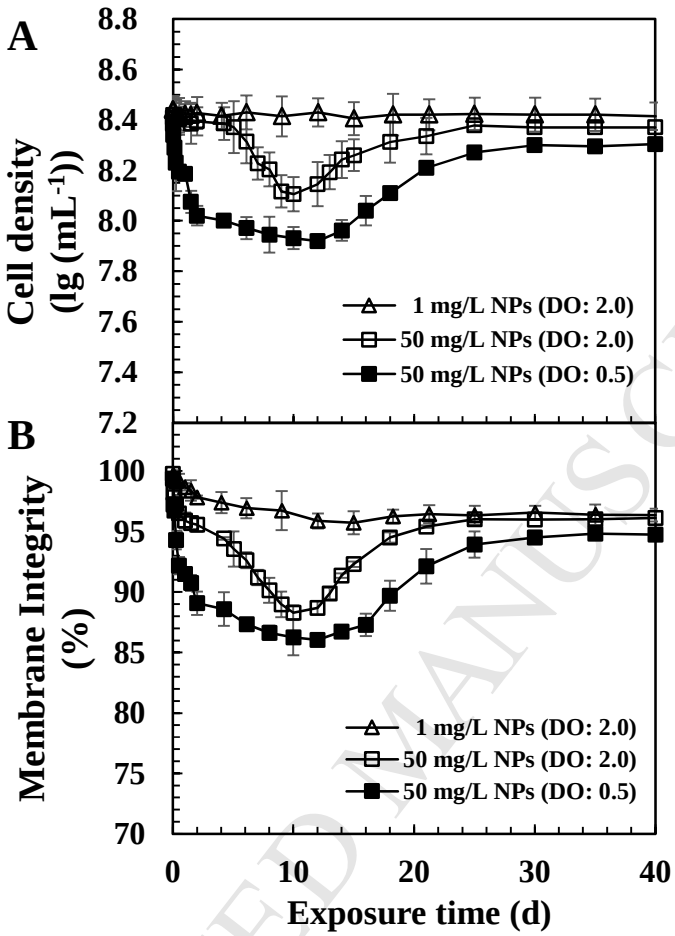

Fig. 2

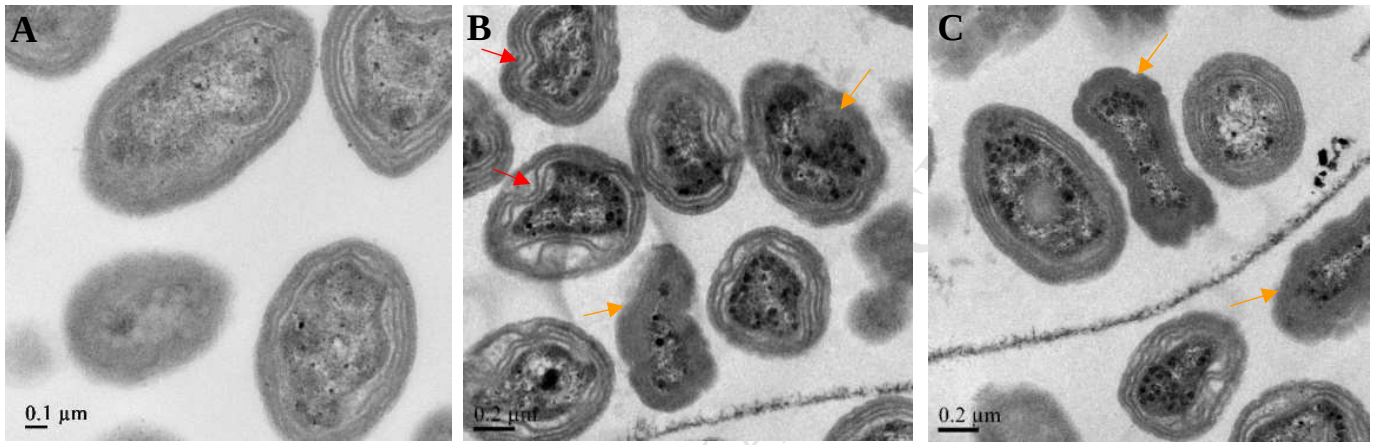

Pre-exposure **12-d exposure** **40-d exposure**

Fig. 3

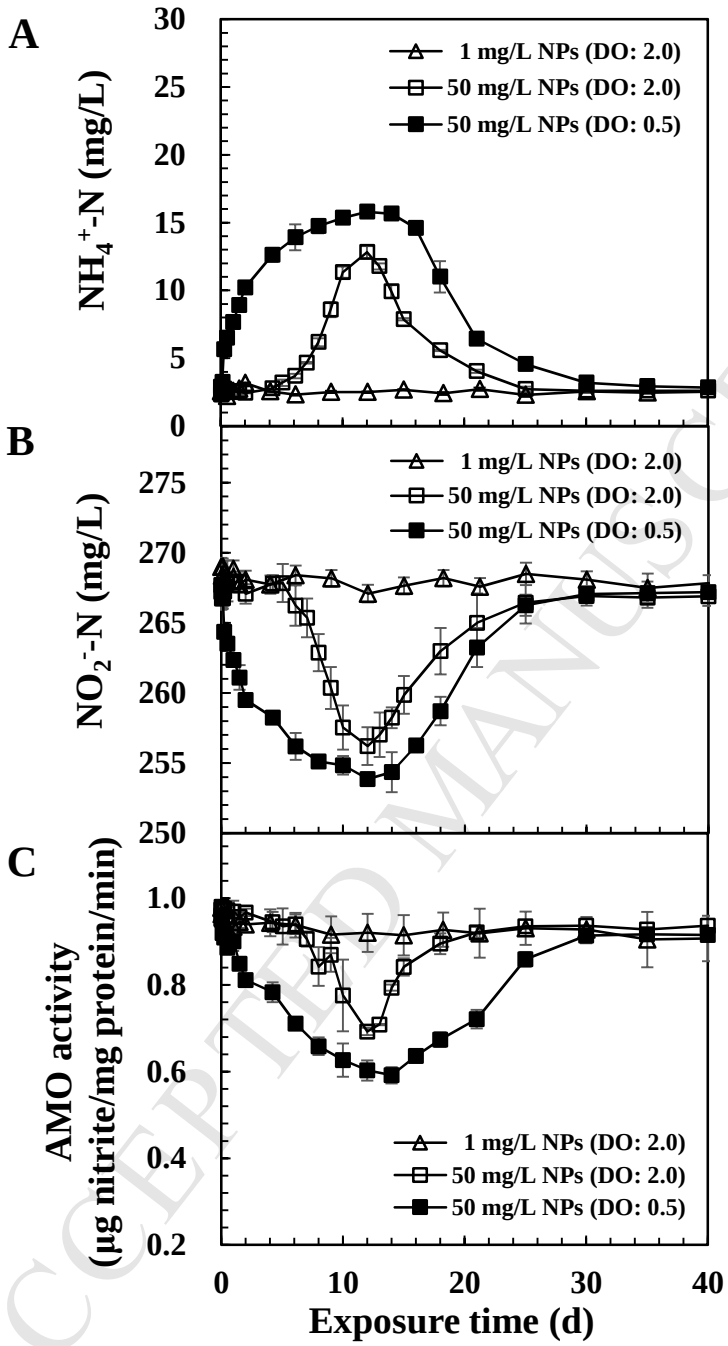

20 **Fig. 4**

21

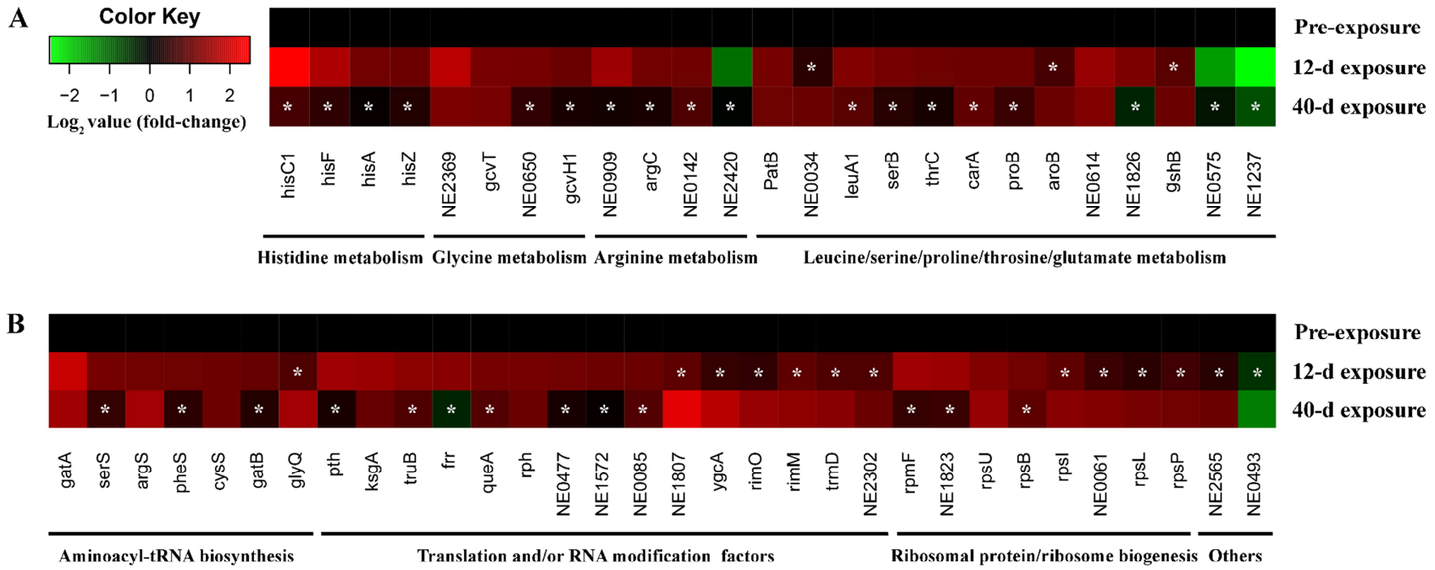

22

23 **Fig. 5**

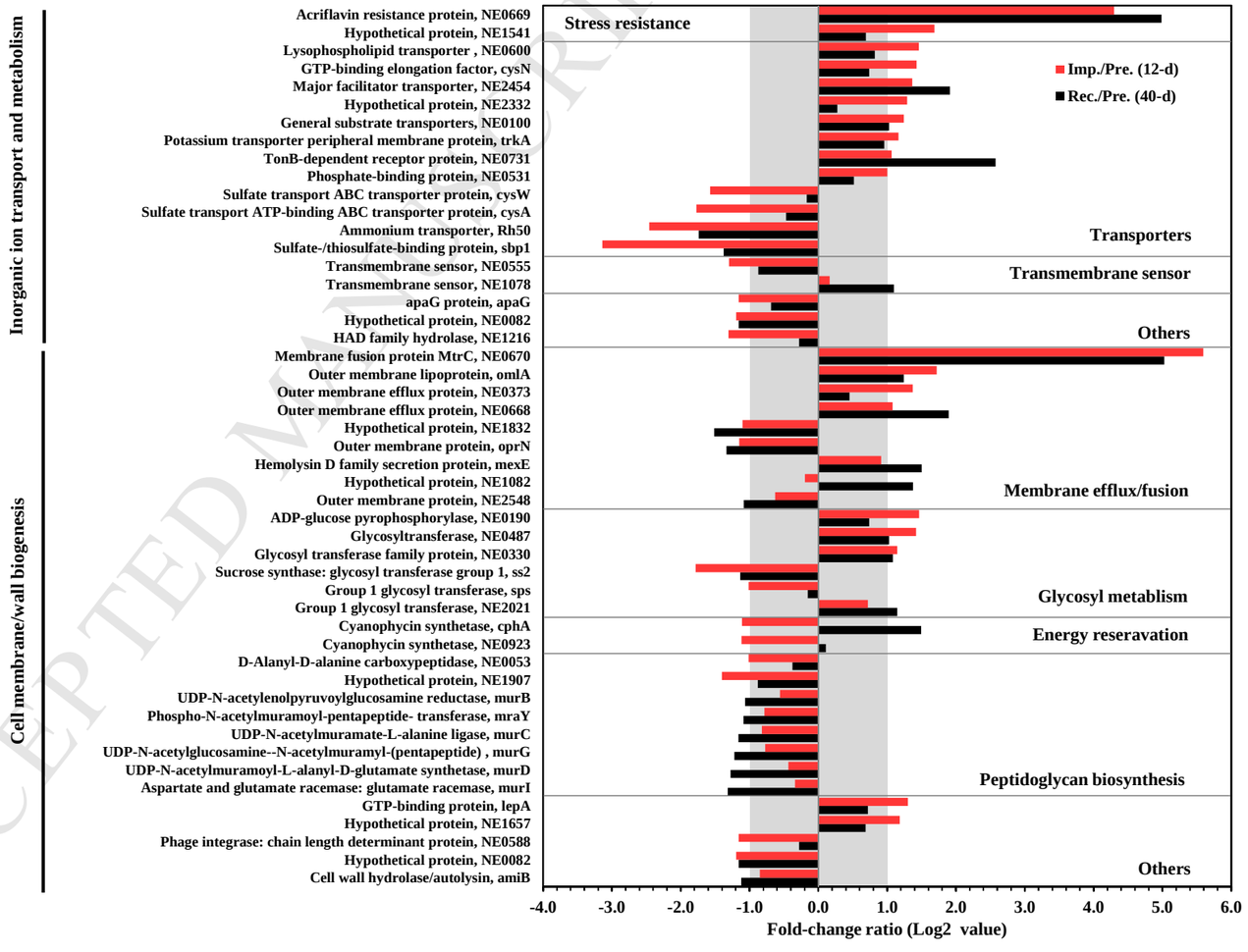

24

Fig. 6

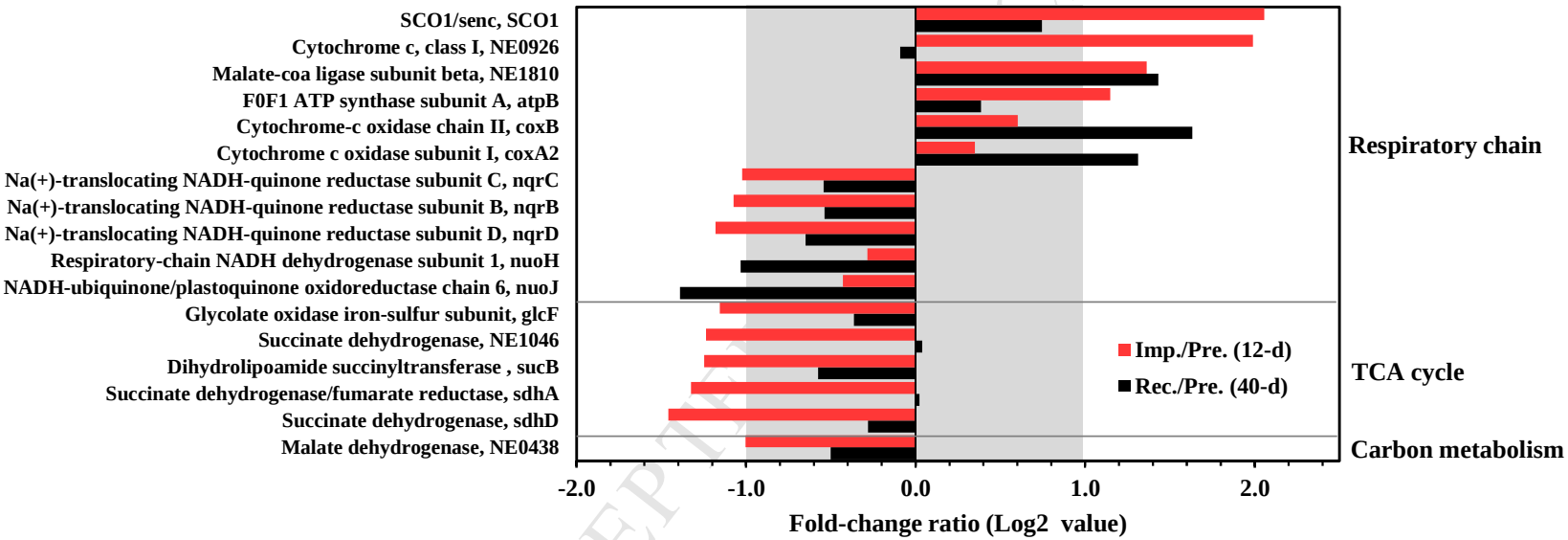
SCO1/senc, SCO1
Cytochrome c, class I, NE0926
Malate-coa ligase subunit beta, NE1810
F0F1 ATP synthase subunit A, atpB
Cytochrome-c oxidase chain II, coxB
Cytochrome c oxidase subunit I, coxA2
Na(+)-translocating NADH-quinone reductase subunit C, nqrC
Na(+)-translocating NADH-quinone reductase subunit B, nqrB
Na(+)-translocating NADH-quinone reductase subunit D, nqrD
Respiratory-chain NADH dehydrogenase subunit 1, nuoH
NADH-ubiquinone/plastoquinone oxidoreductase chain 6, nuoJ
Glycolate oxidase iron-sulfur subunit, glcF
Succinate dehydrogenase, NE1046
Dihydrolipoamide succinyltransferase , sucB
Succinate dehydrogenase/fumarate reductase, sdhA
Succinate dehydrogenase, sdhD
Malate dehydrogenase, NE0438
Imp./Pre. (12-d)
Rec./Pre. (40-d)
Respiratory chain
TCA cycle
Carbon metabolism
-2.0
-1.0
0.0
1.0
2.0
Fold-change ratio (Log2 value)

Adaption and recovery of *Nitrosomonas europaea* to chronic TiO_2 nanoparticle exposure

Research Highlights:

- Cells adapted to chronic NP stress and all the metabolic activities recovered.
- Membrane repair associated regulations were pivotal for cellular adaption.
- Diverse metabolic and stress-defense pathways were activated for cell recovery.
- Low DO condition compromised NP impaired cells' resistance and adaption capacities.
- Stimulation limitation of respiratory chain accounted for the compromised capacity.